

Thermoelectric Power of Lattice Vacancies in Gold*

R. P. HUEBENER

Argonne National Laboratory, Argonne, Illinois

(Received 15 April 1964)

The change ΔS of the thermoelectric power of high-purity gold wires due to quenched-in lattice vacancies was measured between 4.2 and 220°K. The vacancy concentration was determined from the quenched-in electrical resistance at 4.2°K. From the value of ΔS at 200°K, where phonon-drag effects are negligible, the electronic part ΔS_e of ΔS was calculated as a function of the temperature, using the Friedel theory. The phonon-drag part ΔS_g was obtained from the equation $\Delta S_g = \Delta S - \Delta S_e$. Vacancies were found to cause a reduction of the electronic part and of the phonon-drag part of the thermoelectric power. $|\Delta S_e|$ and $|\Delta S_g|$ reach a maximum at low temperatures. The phonon-scattering cross section of vacancies, as estimated from ΔS_g assuming a pure Rayleigh-type scattering mechanism, indicates that phonons are scattered by vacancies predominantly through the strain field associated with the vacant lattice site.

I. INTRODUCTION

THE influence of point defects on the thermoelectric power of a pure metal has been measured recently with dilute alloys of copper¹ and of potassium.² These experiments have shown that, besides changing the electronic component of the thermoelectric power, point defects reduce the phonon-drag component if their phonon-scattering cross section is sufficiently large. Thermoelectric measurements with metals containing impurities provide, therefore, information on the phonon-scattering properties of these imperfections.

In the present investigation the change ΔS of the thermoelectric power of high-purity gold wires due to quenched-in lattice vacancies is measured between 4.2 and 220°K. From the results the electronic component and the phonon drag component of the change in the thermoelectric power is calculated as a function of the temperature. In Sec. II the theoretical treatment of the influence of point defects on the thermoelectric power is summarized. A simple derivation of the electronic component of ΔS , given by de Vroomen³ and by Gold *et al.*⁴ is extended to the phonon-drag component. Sections III and IV give a description of the experiments. In Sec. V the relaxation time τ_i of phonon scattering by lattice vacancies is estimated from the phonon-drag component of ΔS . The relaxation time τ_i and the electronic component of ΔS are compared with theoretical results.

II. THEORY

The absolute thermoelectric power S^0 of a pure metal consists of a contribution S_e^0 , arising from the non-equilibrium distribution of the conduction electrons, and a contribution S_g^0 , caused by the interaction between the conduction electrons and the phonons, which are

not in equilibrium:

$$S^0 = S_e^0 + S_g^0. \quad (1)$$

S_e^0 and S_g^0 are usually called electronic thermoelectric power and phonon-drag thermoelectric power, respectively. The change ΔS in the thermoelectric power of a metal due to impurities is according to Eq. (1)

$$\Delta S = \Delta S_e + \Delta S_g, \quad (2)$$

where ΔS_e and ΔS_g are the change in the electronic and the phonon-drag thermoelectric power, respectively.

A. Change of the Electronic Component of the Thermoelectric Power Due to Point Defects

As pointed out by de Vroomen³ and by Gold *et al.*,⁴ ΔS_e can be derived in a simple way under the following assumptions:

1. The scattering of electrons by an impurity and all other electron scattering events in the crystal are independent of each other (Matthiessen's rule). This implies that the Fermi surface of the material is not changed by the presence of the impurities, and that the impurities are randomly distributed.

2. The heat which is transported by the conduction electrons is independent of other heat transporting mechanisms (phonons).⁵

3. The electron scattering in the material can be treated in terms of a single isotropic group of charge carriers.

Under the assumptions 1–3, the electronic part W_e of the thermal resistance of a metal containing imperfections is the sum of the resistance W_e^0 of the pure material and the resistance ΔW_e of the imperfections

$$W_e = W_e^0 + \Delta W_e. \quad (3)$$

We divide a small temperature difference ΔT across the specimen in two parts according to the thermal resist-

* Based on work performed under the auspices of the U. S. Atomic Energy Commission.

¹ F. J. Blatt and R. H. Kropschot, Phys. Rev. **118**, 480 (1960).

² A. M. Guénault and D. K. C. MacDonald, Proc. Roy. Soc. (London) **A264**, 41 (1961).

³ A. R. de Vroomen, thesis, University of Leiden, 1959 (unpublished).

⁴ A. V. Gold, D. K. C. MacDonald, W. B. Pearson, and I. M. Templeton, Phil. Mag. **5**, 765 (1960).

⁵ This requirement is formulated in a more general way as in the paper by Gold *et al.* (see Ref. 4).

ances W_e^0 and ΔW_e :

$$\Delta T = \frac{W_e^0}{W_e^0 + \Delta W_e} \Delta T + \frac{\Delta W_e}{W_e^0 + \Delta W_e} \Delta T. \quad (4)$$

The thermoelectric potential difference across the specimen is then given by the sum

$$\Delta V_e = S_e^0 \frac{W_e^0}{W_e^0 + \Delta W_e} \Delta T + S_e^i \frac{\Delta W_e}{W_e^0 + \Delta W_e} \Delta T, \quad (5)$$

where S_e^i is the electronic thermoelectric power of the imperfections in the metal.

If the scattering potential associated with the impurities is isotropic, the quantity S_e^i is given by the electronic thermoelectric power of a single impurity. In the case of an anisotropic scattering potential S_e^i is the electronic thermoelectric power of a single impurity averaged over all impurity orientations within the crystal.

From Eq. (5) we find the total electronic thermoelectric power S_e of a metal containing impurities:

$$S_e = \frac{W_e^0}{W_e^0 + \Delta W_e} S_e^0 + \frac{\Delta W_e}{W_e^0 + \Delta W_e} S_e^i. \quad (6)$$

Equation (6) was derived originally by Kohler⁶ from a variational solution of the Boltzmann equation. From Eq. (6) we obtain

$$\Delta S_e \equiv S_e - S_e^0 = \frac{S_e^0}{(W_e^0/\Delta W_e) + 1} \left(\frac{S_e^i}{S_e^0} - 1 \right). \quad (7)$$

If we require in addition to the assumptions 1-3, mentioned above, that the electrical conductivity and the electronic component of the heat conductivity are determined by the same relaxation time (Wiedemann-Franz law), Eq. (7) can be replaced by

$$\Delta S_e = \frac{S_e^0}{(\rho_0/\Delta\rho) + 1} \left(\frac{S_e^i}{S_e^0} - 1 \right). \quad (8)$$

ρ_0 and $\Delta\rho$ are the electrical resistivity of the pure metal and of the imperfections, respectively.

Equation (8) can also be derived, of course, from the expression for S_e^0 , which is obtained from the solution of the Boltzmann equation in the case of an electrical field and a temperature gradient. With the same assumptions which have led to Eq. (8), the Boltzmann equation yields for the electronic thermoelectric power of a pure metal⁷

$$S_e^0 = \frac{\pi^2 k_B^2 T}{3e} \left(\frac{1}{\rho_0} \frac{\partial \rho_0(E)}{\partial E} \right)_{E_F}, \quad (9)$$

where k_B is Boltzmann's constant, T the absolute temperature, e the absolute value of the elementary charge, E the energy of the conduction electrons, and E_F the Fermi energy. The total electronic thermoelectric power of a metal containing imperfections is found from Eq. (9) by replacing ρ_0 with $\rho_0 + \Delta\rho$. In this way one obtains⁸

$$\Delta S_e = \frac{S_e^0}{(\rho_0/\Delta\rho) + 1} \left[\frac{(1/\Delta\rho)(\partial\Delta\rho/\partial E)}{(1/\rho_0)(\partial\rho_0/\partial E)} - 1 \right]_{E_F}. \quad (10)$$

Since the factor

$$\left[\frac{(1/\Delta\rho)(\partial\Delta\rho/\partial E)}{(1/\rho_0)(\partial\rho_0/\partial E)} - 1 \right]_{E_F}$$

is independent of the temperature, the temperature dependence of ΔS_e is determined by the function

$$G = S_e^0 / [(\rho_0/\Delta\rho) + 1]. \quad (11)$$

According to Eqs. (9) and (10), the measurement of ΔS_e yields information on the derivative $(\partial\Delta\rho/\partial E)_{E_F}$, provided the quantities S_e^0 , ρ_0 , and $\Delta\rho$ are known. The change of the electrical resistance caused by imperfections is given by⁷

$$\Delta\rho = 3N_i \sigma(E) / 2e^2 n(E) v(E). \quad (12)$$

Here N_i is the number of imperfections per volume, σ the momentum transfer cross section of the imperfections for electron scattering, n the density of electron states, and v the velocity of the electrons. From Eq. (12) we obtain

$$\frac{1}{\Delta\rho} \frac{\partial \Delta\rho}{\partial E} = \frac{1}{\sigma} \frac{\partial \sigma(E)}{\partial E} - \frac{1}{nv} \frac{\partial [n(E)v(E)]}{\partial E}. \quad (13)$$

According to Eq. (13) the quantity $(\partial\Delta\rho/\partial E)_{E_F}$ yield information on the derivative $(\partial\sigma/\partial E)_{E_F}$, provided the functions $n(E)$ and $v(E)$ are known.

B. Change of the Phonon-Drag Component of the Thermoelectric Power due to Point Defects

For evaluating ΔS_e we may use the same arguments for the phonon system, which we have used above for the electron system and which have led to Eq. (7). In analogy to the assumptions on the electrons, we require the following simplifications on the phonon system:

1. The scattering of phonons by an impurity and all other phonon-scattering events in the crystal are independent of each other (Matthiessen's rule). This implies, that the phonon spectrum is not changed by the presence of the imperfections, and that the impurities are randomly distributed.

2. The heat which is transported by the phonons is

⁶ M. Kohler, Z. Physik **126**, 481 (1949).

⁷ A. H. Wilson, *The Theory of Metals* (Cambridge University Press, New York, 1953).

⁸ J. Friedel, J. Phys. Radium **14**, 561 (1953).

independent of other heat transporting mechanisms (electrons). This requirement is valid in the temperature range, where electron-phonon collisions are negligible compared to other phonon scattering mechanisms (phonon-impurity and phonon-phonon interactions).

Since the entire frequency spectrum of the phonon system contributes to the transport phenomena, and because of the frequency dependence of the scattering processes, the analogy of assumption 3 in Sec. IIA is not valid. We have to treat phonons with a different magnitude of the wave vector separately. Under the assumptions 1 and 2 the lattice resistance for phonons with the wave vector \mathbf{q} and the polarization j in a metal containing impurities is the sum of the lattice resistance of the pure material and the resistance of the imperfections. We separate a small temperature difference ΔT across the specimen, as seen by phonons of the type \mathbf{q}, j , in two parts according to the inverse relaxation times of the participating scattering processes.

$$\Delta T_{\mathbf{q},j} = \frac{1/\tau_0(\mathbf{q},j)}{[1/\tau_0(\mathbf{q},j)] + [1/\tau_i(\mathbf{q},j)]} \Delta T_{\mathbf{q},j} + \frac{1/\tau_i(\mathbf{q},j)}{[1/\tau_0(\mathbf{q},j)] + [1/\tau_i(\mathbf{q},j)]} \Delta T_{\mathbf{q},j}$$

or

$$\Delta T_{\mathbf{q},j} = \frac{1}{1 + [\tau_0(\mathbf{q},j)/\tau_i(\mathbf{q},j)]} \Delta T_{\mathbf{q},j} + \frac{1}{1 + [\tau_i(\mathbf{q},j)/\tau_0(\mathbf{q},j)]} \Delta T_{\mathbf{q},j}. \quad (14)$$

$\tau_0(\mathbf{q},j)$ and $\tau_i(\mathbf{q},j)$ are the relaxation time of the phonon scattering by the host material and by the impurities, respectively.

The phonons which are scattered by the impurities do not contribute to the phonon-drag part of the thermoelectric potential difference across the specimen. According to Eq. (14) the thermoelectric potential difference caused by phonons of the type \mathbf{q}, j is therefore given by

$$\Delta V_{\mathbf{q},j} = \frac{s_g(\mathbf{q},j) \Delta T_{\mathbf{q},j}}{1 + [\tau_0(\mathbf{q},j)/\tau_i(\mathbf{q},j)]}, \quad (15)$$

where s_g is the phonon drag thermoelectric power of the host material associated with the phonons \mathbf{q}, j . By integrating over all phonons and by writing the phonon drag thermoelectric power of the pure material as

$$S_g^0 = \sum_j \int s_g(\mathbf{q},j) d^3q, \quad (16)$$

we find from Eq. (15) the phonon-drag thermoelectric power of a metal containing imperfections:

$$S_g = \sum_j \int \frac{s_g(\mathbf{q},j)}{1 + [\tau_0(\mathbf{q},j)/\tau_i(\mathbf{q},j)]} d^3q. \quad (17)$$

From Eqs. (16) and (17) we obtain

$$\Delta S_g \equiv S_g - S_g^0 = - \sum_j \int \frac{s_g(\mathbf{q},j)}{1 + [\tau_i(\mathbf{q},j)/\tau_0(\mathbf{q},j)]} d^3q. \quad (18)$$

Equation (18) corresponds to Eq. (7) for the electronic part of the thermoelectric power. According to Eq. (18) the phonon-drag thermoelectric power is reduced by the presence of imperfections. The reduction depends on the ratio of the relaxation time of the phonon scattering by the impurities and by the host material.

An expression for the phonon drag thermoelectric power which contains both the normal and the umklapp interaction between electrons and phonons has been derived by Bailyn^{9,10} for the general case of a non-spherical Fermi surface and several bands. For a cubic crystal with a single band of standard form Bailyn obtained

$$S_g^0 = \frac{1}{3eN_e T} \frac{12\pi^3 \hbar}{\Delta_0 \cdot B \cdot v(E_F)} \sum_{\mathbf{q},j} \frac{ze^z}{(e^z - 1)^2} \sum_{\mathbf{k},\mathbf{k}'}^{[\mathbf{q},j]} \alpha(\mathbf{q},j; \mathbf{k},\mathbf{k}') \times \nabla_{\mathbf{q}\omega} \cdot [\mathbf{v}(\mathbf{k}) - \mathbf{v}(\mathbf{k}')]. \quad (19)$$

Here e is the absolute value of the elementary charge, N_e the number of conduction electrons of the specimen, \hbar Planck's constant, and Δ_0 the atomic volume of the metal. B is the area of the Fermi surface, and $v(E_F)$ the average velocity on the Fermi surface. $\mathbf{v}(\mathbf{k})$ is the velocity of the electrons with the wave vector \mathbf{k} . The parameter z is given by

$$z = \hbar\omega(\mathbf{q},j)/k_B T, \quad (20)$$

where $\omega(\mathbf{q},j)$ is the frequency of the phonon \mathbf{q}, j . $\alpha(\mathbf{q},j; \mathbf{k},\mathbf{k}')$ is the relative probability that a phonon \mathbf{q}, j will be emitted or absorbed in a $\mathbf{k} \leftrightarrow \mathbf{k}'$ transition of the electrons

$$\alpha(\mathbf{q},j; \mathbf{k},\mathbf{k}') = \left[\frac{1}{\tau_{ep}(\mathbf{k},\mathbf{k}')} \right] / \left[\sum_l \frac{1}{\tau_l} + \sum_{\mathbf{k},\mathbf{k}'}^{[\mathbf{q},j]} \frac{1}{\tau_{ep}(\mathbf{k},\mathbf{k}')} \right]. \quad (21)$$

τ_{ep} is the relaxation time of the electron-phonon interactions. τ_l are the relaxation times of any phonon-scattering processes not involving electrons. The sums in Eq. (19) and in the denominator of Eq. (21) are over all transitions $\mathbf{k} \leftrightarrow \mathbf{k}'$ in which the emission or absorption of the particular phonons \mathbf{q}, j is allowed by the selection rule

$$\mathbf{k}' - \mathbf{k} = \mathbf{q} + \mathbf{K}, \quad (22)$$

where \mathbf{K} is a reciprocal lattice vector.

In the case of a normal band (positive effective electron mass) of standard form we have $\mathbf{v} \sim \mathbf{k}$. With $\nabla_{\mathbf{q}\omega} \sim \mathbf{q}$ and with the selection rule (22) we find

$$\nabla_{\mathbf{q}\omega} \cdot [\mathbf{v}(\mathbf{k}) - \mathbf{v}(\mathbf{k}')] \sim -\mathbf{q}(\mathbf{q} + \mathbf{K}). \quad (23)$$

⁹ M. Bailyn, Phil. Mag. **5**, 1059 (1960).

¹⁰ M. Bailyn, Phys. Rev. **120**, 381 (1960).

According to Eqs. (19) and (23) the contribution of normal processes ($\mathbf{K}=0$) to S_e^0 is negative. The contribution of umklapp processes ($\mathbf{K}\neq 0$) to S_e^0 is in general positive.

In the case of an inverted band (negative effective electron mass) of standard form we have $\mathbf{v}\sim-\mathbf{k}$. Normal processes are then found to give a positive contribution to S_e^0 , whereas umklapp processes yield in general a negative contribution.

C. Separation of the Electronic Component and the Phonon-Drag Component of ΔS

The experimentally determined quantity ΔS can be separated into ΔS_e and ΔS_p using the following arguments about the temperature dependence of the electronic component and of the phonon-drag component of the thermoelectric power. At high temperatures, S_e^0 and ΔS_p become negligible because of the dominant influence of phonon scattering processes, which do not involve electrons [Eqs. (19) and (21)]. Therefore, the value of ΔS at high temperatures is equal to ΔS_e . It can be used to calculate ΔS_e as a function of the temperature from Eq. (10), provided the temperature dependence of the function G given in Eq. (11) has been determined.

Whereas $\rho_0/\Delta\rho$ in G can be obtained as a function of the temperature directly from measurements, $S_e^0(T)$ is derived from the absolute thermoelectric power $S^0(T)$ in the following way. As shown in Fig. 1, the absolute thermoelectric power of pure gold increases rapidly with increasing temperature for temperatures higher than about 10°K. It passes then through a maximum and, above a temperature of about 200°K, increases linearly with increasing temperature. The high-temperature branch of S^0 extrapolates linearly to the origin. Since S_e^0 is linear-dependent on the temperature according to Eq. (9) and since S_p^0 vanishes at high temperatures, the curve obtained by extrapolating the

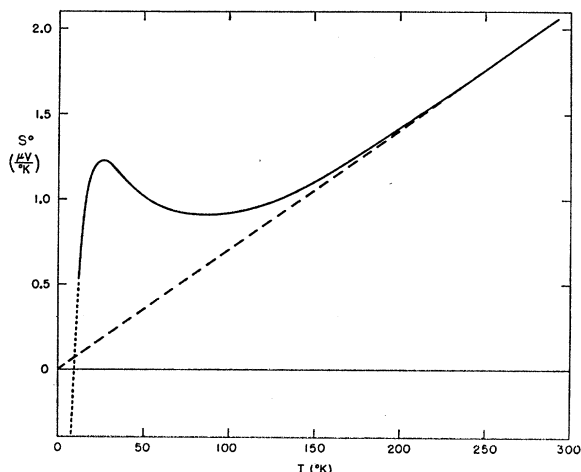


FIG. 1. Absolute thermoelectric power of gold versus temperature.

high-temperature branch of $S^0(T)$ linearly to the origin is interpreted as the electronic component $S_e^0(T)$. The difference between this linear curve and $S^0(T)$ is interpreted as the phonon-drag component $S_p^0(T)$.

After determining in this way the function G , the electronic component ΔS_e is calculated as a function of the temperature from Eq. (10). The phonon drag component $\Delta S_p(T)$ is obtained from Eq. (2).

III. EXPERIMENTAL PROCEDURE

A. Sample Preparation

The specimen material was polycrystalline 99.999% pure gold wire of 0.010-in. diam.¹¹ The specimen, shown in Fig. 2, consisted of a center wire and two potential lead wires mounted on a stainless-steel sample holder. The specimen wires were spot-welded to short pieces of 0.016-in.-diam gold wire which were attached to the sample holder. The center wire was electrically connected with both potential lead wires by two gold wires of 0.002-in. diameter and of about 0.5-cm length. The potential lead wires were arranged to cross the center wire near these electrical connections to provide the possibility for spot-welding the wires together after the quenching procedure. They were bent as indicated in Fig. 2 to obtain a good thermal contact with the heat sink inside the cryostat. The length of the center wire between the potential lead wires was about 6 cm. All gold wires used in assembling the specimen were 99.999% pure.¹¹

After mounting, each of the specimen wires was annealed in air for 1 h at 750°C by passing direct current through it and cooled gradually to room temperature. The electrical resistance of the part of the center wire between both potential leads was then measured at room temperature and in a bath of liquid nitrogen and of liquid helium using the following procedure. A dc current of about 30 mA passed through the specimen wire and through a $1.0000 \times 10^{-2} \Omega$ resistance standard which was held at room temperature. The resistance was calculated from the ratio of the voltage drop across the specimen wire and the standard resistance. The resistance measurements at 4.2 and at 77.3°K were carried out using a Rubicon model 2768 microvolt potentiometer and a Rubicon model 3550 photoelectric galvanometer. For the resistance measurements at room temperature a Leeds and Northrup K-3 potentiometer was used. Errors in the voltage readings due to thermoelectric effects within the circuitry were eliminated by reversing the current. The ratio of the resistance of the annealed specimens at room temperature to that at 4.2°K was between 1150 and 1400.

For quenching, the sample holder was attached to a pivot joint and placed over a tank filled with ice water. The center wire was heated by passing direct current through it. The distance between the heated wire and

¹¹ Obtained from the Sigmund Cohn Corporation, Mount Vernon, New York.

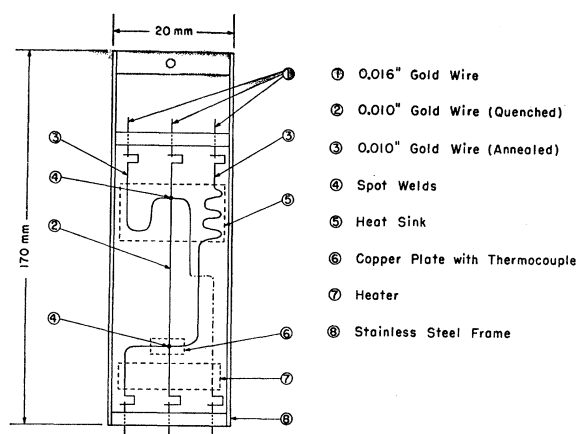


FIG. 2. Scheme of the specimen.

the water was 0.5 cm. The specimen was shielded from drafts by a plexiglass cover. By optical pyrometry the temperature of the heated wire was found to be uniform within $\pm 2\%$ over the length between both potential leads. The quench temperature was obtained from the ratio of the electrical resistance at high temperature to that at room temperature in combination with a resistance temperature calibration. The electrical resistance of the heated wire was measured immediately before quenching using a Honeywell model 906C multi-channel recording oscillograph connected with the potential leads. The heating current, which also passed through a resistance standard, was determined simultaneously with the voltage drop across the heated wire using a second channel of the oscillograph. Quenching was performed by driving the sample holder into the water after releasing a spring. The experiments were carried out with quench temperatures between 780 and 930°C. As indicated by the oscillograph, the temperature of the heated wire dropped about linearly with time to the water temperature within $(4.5 \pm 1.2) \times 10^{-2}$ sec corresponding to quench rates of about 2×10^4 °C/sec. Immediately after the specimen had entered the water the heating current was turned off.

By quenching, lattice vacancies, which are thermally produced at the high temperature, are trapped within the crystal. During the time necessary to cool the specimen, monovacancies, which are predominant at high temperatures, can coagulate forming divacancies and larger vacancy clusters.^{12,13} The extent to which polyvacancies were formed in the specimens during quenching can be estimated from the theoretical studies of Koehler, Seitz, and Bauerle¹⁴ and Cotterill¹⁵ on the influence of the quench temperature and the

quench rate on the coagulation of monovacancies in gold. The calculations of these authors indicate, using a binding energy of a divacancy in gold of 0.1 eV,¹² that with the quench temperatures and the quench rate mentioned above predominantly monovacancies were obtained.

After quenching, the specimen was rinsed with methylalcohol. The 0.002-in.-diam gold wires connecting the center wire and the potential lead wires were cut off. Both potential lead wires were then spot-welded to the center wire at the crossing points and the specimen was assembled in the cryostat. Before the vacuum can of the cryostat was mounted, the sample was cooled to liquid-nitrogen temperatures. The specimens were kept at room temperature for less than 30 min after quenching. After sealing the vacuum can with Woods metal the cryostat was filled with helium gas and immersed into liquid nitrogen. To determine the quenched-in vacancy concentration the electrical resistance of the quenched wire was measured within the cryostat at 4.2°K. In order to correct for small changes of the specimen length caused by replacing the 0.002-in.-diam wire connections with direct spot welds, the resistance of the center wire was measured again at room temperature within the cryostat after completion of the thermoelectric measurements.

B. Cryostat

The assembly of the specimen within the cryostat is shown in Fig. 3. The cryostat contained a thin-walled stainless steel tube which was open at the top and which was joined with an elbow at the bottom. A copper plate with a thickness of 3.5 mm soldered to the end of the elbow provided the thermal ground inside the cryostat. The sample holder was attached to an extension of the copper plate. The area of the heat sink indicated in

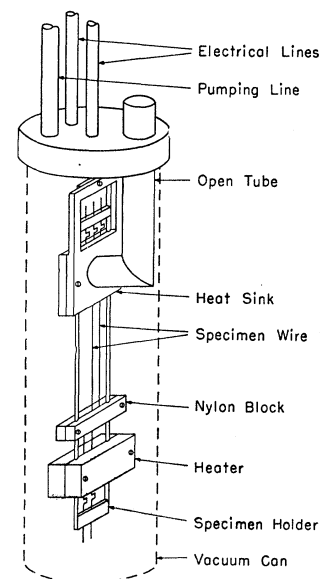


FIG. 3. Specimen assembly.

¹² M. de Jong and J. S. Koehler, Phys. Rev. **129**, 40 (1963).

¹³ M. de Jong and J. S. Koehler, Phys. Rev. **129**, 49 (1963).

¹⁴ J. S. Koehler, F. Seitz, and J. E. Bauerle, Phys. Rev. **107**, 1499 (1957).

¹⁵ R. M. J. Cotterill (to be published). The author is grateful to Dr. Cotterill for providing him with the results prior to publication.

Fig. 2 coincided with the surface of the copper plate. The specimen wire was held against the thermal ground by a second copper plate screwed on. The heater consisted of two copper blocks carrying manganin heating wires. The copper blocks were clamped from both sides against the specimen wire below the lower (hot) junction of the quenched and the annealed gold wire. The copper plates covering the upper (cold) junction of the quenched and the annealed gold wire and the copper blocks of the heater were insulated from the specimen wire by a thin layer of GE No. 7031 varnish coated with vacuum grease. After assembling the sample holder in the cryostat, the part of the annealed gold wire, which is indicated by a dashed line in Fig. 2, was cut off.

Two small copper plates, which were attached to two nylon blocks, and which were coated with GE No. 7031 varnish and vacuum grease, were clamped against the lower junction of the quenched and the annealed gold wire. The temperature of the lower junction was measured by a gold 2.1% cobalt versus copper thermocouple¹¹ attached to one of the small copper plates. The other junction of this thermocouple was attached to the inside of the copper plate covering the specimen at the thermal ground. The thermocouple wire had a diameter of 0.003 in. It was electrically insulated from the specimen wire and from the copper plates by thin layers of GE No. 7031 varnish. The thermocouple voltage was measured with a Leeds and Northrup K-3 potentiometer. The temperature difference between both thermocouple junctions was obtained from the table of Powell *et al.*¹⁶ The thermocouple wire was checked at the temperatures of liquid helium, liquid nitrogen, and ice water. The thermoelectric voltage was found to deviate by less than 0.2% from the data obtained from the table of Powell *et al.*¹⁶ for these temperatures.

Liquid helium or liquid nitrogen was used as a temperature bath. The cooling liquid inside the open stainless steel tube of the cryostat provided the thermal ground for the upper junction of the specimen wires and the gold 2.1% cobalt versus copper thermocouple. Upon heating the lower junction of the specimen wires the temperature of the upper junction rose slightly above the temperature of the cooling liquid. In an experiment with an annealed specimen, this temperature shift was measured using an additional thermocouple spot-welded to the specimen wire. With liquid nitrogen as the temperature bath the temperature shift of the upper junction was 1.0% of the temperature difference between both junctions. Above 20°K with liquid helium as the temperature bath the temperature shift of the upper junction was 2.9% of the temperature difference between both junctions, below 20°K it was somewhat larger.

The annealed specimen wires were spot-welded to

extensions of annealed 99.999% pure gold wire¹¹ leading out of the low-temperature bath.

C. Thermoelectric Measurements

During the thermoelectric measurements the cryostat was evacuated to less than 10^{-6} mm Hg. The thermoelectric voltage of the thermocouple, consisting of the quenched and the annealed gold wire, was measured with the same potentiometer used for the resistance measurements at 4.2 and 77.3°K. With this equipment voltage changes of $0.01 \mu\text{V}$ could be detected. The thermoelectric voltage was measured as a function of the temperature of the hot junction keeping the cold junction at the temperature of the cooling bath. For the measurements in the temperature interval between 4.2 and 80°K the cryostat was placed in liquid helium. During the measurements in the temperature range between 77.3 and 220°K the cryostat was immersed in liquid nitrogen. The temperature of the hot junction of the sample was changed by less than 0.3°K per minute. The same results were obtained with rising and with falling temperature of the hot junction. The data were taken at temperature intervals of 1°K at temperatures below 130°K and at somewhat larger intervals at higher temperatures.

The thermoelectric power was obtained by differentiating the voltage-temperature curves with respect to the temperature using an IBM-704 computer. A quadratic function was fitted by the method of least squares to six neighboring points with the additional requirement that the function, obtained for the total range of the data, and its first and second derivative were continuous.

IV. EXPERIMENTAL RESULTS

The change ΔS of the thermoelectric power of gold wire caused by quenched-in lattice vacancies is shown in Fig. 4 as a function of the temperature for different vacancy concentrations. At temperatures above about 10°K vacancies reduce the thermoelectric power. $|\Delta S|$ passes through a maximum between 15 and 20°K and at higher temperatures decreases with increasing temperature. Above 150°K, ΔS was found to be independent of the temperature for the vacancy concentrations studied. The vacancy concentrations given in the caption of Fig. 4 and hereafter are calculated from the quenched-in electrical resistivity $\Delta\rho$, assuming $\Delta\rho$ is caused by monovacancies with a resistivity of $1.8 \times 10^{-6} \Omega\text{cm/at. \%}$.¹⁷ In Fig. 5, ΔS at 200°K is shown as a function of the quenched-in electrical resistivity $\Delta\rho$. At 200°K $|\Delta S|$ increases linearly with $\Delta\rho$. For small vacancy concentrations c the data given in Fig. 5 yield the relation

$$(\Delta S/c)_{200^\circ\text{K}} = -1.67 \pm 0.03 \mu\text{V}/^\circ\text{K at. \%}. \quad (24)$$

¹⁶ R. L. Powell, M. D. Bunch, and R. J. Corruccini, *Cryogenics* **1**, 1 (1961).

¹⁷ R. P. Huebener and C. G. Homan, *Phys. Rev.* **129**, 1162 (1963).

The thermoelectric voltage measured with a specimen which had not been quenched after annealing corresponded to a value of $|\Delta S|$ of about $1 \times 10^{-2} \mu\text{V}/^\circ\text{K}$ at temperatures between 20 and 70°K and to a somewhat larger value at temperatures below 20°K. Above liquid-nitrogen temperatures, this specimen produced a thermoelectric signal corresponding to a value of $|\Delta S|$ of less than $1 \times 10^{-4} \mu\text{V}/^\circ\text{K}$. Similar results were obtained with a quenched sample which had been annealed for 60 h at room temperature within the cryostat.

The separation of ΔS in the electronic component ΔS_e and the phonon-drag component ΔS_p requires the knowledge of the absolute thermoelectric power of the annealed specimen wire. Therefore, the thermoelectric power of a thermocouple consisting of the annealed specimen wire and high-purity lead wire¹⁸ (99.9999%) was measured as a function of the temperature. The absolute thermoelectric power of the specimen wire, which is shown in Fig. 1, was obtained from the measurements using the data of Borelius *et al.*¹⁹ and of Christian *et al.*²⁰ on the absolute thermoelectric power of lead. The data presented in Fig. 1 are in good agreement with the thermoelectric power of annealed pure gold reported by Pearson.²¹

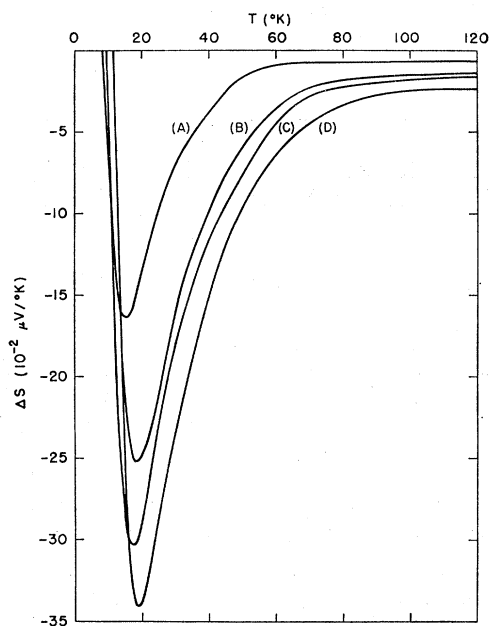


FIG. 4. Change of the absolute thermoelectric power of gold caused by quenched-in vacancies as function of temperature. (A): $c=0.403 \times 10^{-2}$ at. %; (B): $c=0.825 \times 10^{-2}$ at. %; (C): $c=0.865 \times 10^{-2}$ at. %; (D): $c=1.42 \times 10^{-2}$ at. %.

¹⁸ Obtained from Cominco Products, Incorporated, Spokane, Washington.

¹⁹ G. Borelius, W. H. Keesom, C. H. Johansson, and J. O. Linde, Proc. Acad. Sci. Amsterdam 35, 10 (1932).

²⁰ J. W. Christian, J. P. Jan, W. B. Pearson, and I. M. Templeton, Proc. Roy. Soc. (London) A245, 213 (1958).

²¹ W. B. Pearson, Fiz. Tverd. Tela 3, 1411 (1961) [English transl.: Soviet Phys.—Solid State 3, 1024 (1961)].

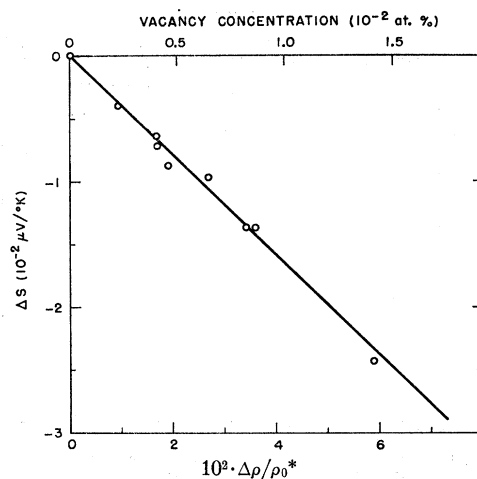


FIG. 5. Change of the thermoelectric power of gold at 200°K due to quenching versus the quenched-in electrical resistivity. ρ_0^* is the annealed resistivity at 77.3°K.

The total change ΔS of the thermoelectric power was separated in ΔS_e and ΔS_p using the method mentioned in Sec. II. To calculate the temperature dependence of the function G given in Eq. (11), the electrical resistivity ρ_0 of the annealed specimen was measured at 4.2, 77.3, and 296°K and was interpolated between these temperatures using the data of Burgers, Cath, and Onnes.²² The resistivity change $\Delta\rho$ measured at 4.2°K was used for all temperatures. The assumed temperature independence of $\Delta\rho$ was checked by measuring the quenched-in electrical resistance of a specimen at 4.2, 77.3, 194.6, and 273.2°K. At the temperatures above 4.2°K, $\Delta\rho$ was slightly larger than at 4.2°K. The maximum deviation from the value of $\Delta\rho$ at 4.2°K was 11%.

The change of the electronic and of the phonon-drag thermoelectric power calculated from the data of Fig. 4 using Eq. (10) is shown in Figs. 6 and 7, respectively, as a function of the temperature for different vacancy concentrations. Above 80°K the change of the electronic thermoelectric power is dominant in ΔS . Below 80°K the change of the phonon-drag thermoelectric power becomes appreciable. It exceeds the change of the electronic contribution at temperatures below 50 to 60°K. Both $|\Delta S_e|$ and $|\Delta S_p|$ pass through a maximum between 15 and 20°K for the vacancy concentrations studied.

In order to estimate the error in calculating the temperature dependence of ΔS_e from Eq. (10), it is necessary to examine the validity of the assumptions leading to this equation. As mentioned above the deviations from Matthiessen's rule were found to be less than 11%. Deviations from the second assumption made in Sec. IIA are negligible since, in pure metals,

²² *International Critical Tables*, edited by E. W. Washburn (McGraw-Hill Book Company, Inc., New York, 1929), Vol. 6, p. 125.

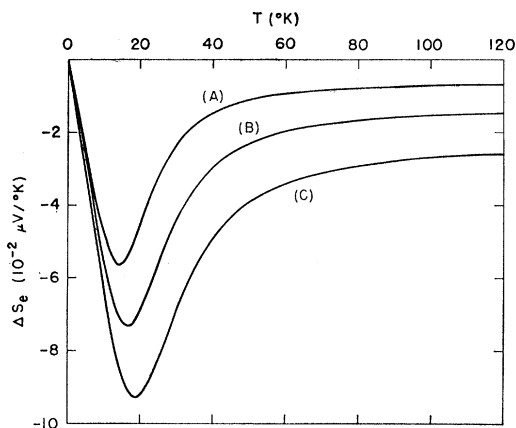


FIG. 6. Change of the electronic thermoelectric power of gold caused by quenched-in vacancies as function of temperature. (A): $c=0.403 \times 10^{-2}$ at.%; (B): $c=0.865 \times 10^{-2}$ at.%; (C): $c=1.42 \times 10^{-2}$ at. %.

heat is dominantly transported by electrons. The Fermi surface of gold deviates from an isotropic distribution²³ assumed in Sec. IIA. However, in a material with an anisotropic Fermi surface the expression for ΔS_e given in Eq. (7) is still valid, provided the quantities ΔW_e and S_e^i are taken as average values over the Fermi surface.

Deviations from the Wiedemann-Franz law occur if the conduction electrons are scattered inelastically. An estimate of the deviation from the Wiedemann-Franz law may be obtained using the experimental values of the thermal conductivity of annealed 99.999% pure gold given by White.²⁴ The Wiedemann-Franz ratio $\kappa\rho_0/T$ (κ =thermal conductivity) was calculated for different temperatures, using the thermal conductivity data of White²⁴ and the electrical resistivity of the annealed specimen of the present work. As seen from

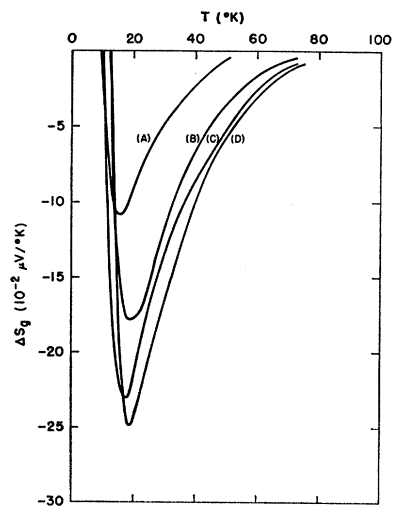


FIG. 7. Change of the phonon-drag thermoelectric power of gold caused by quenched-in vacancies as function of temperature. (A): $c=0.403 \times 10^{-2}$ at.%; (B): $c=0.825 \times 10^{-2}$ at.%; (C): $c=0.865 \times 10^{-2}$ at.%; (D): $c=1.42 \times 10^{-2}$ at. %.

²³ J. M. Ziman, *Advan. Phys.* **10**, 1 (1961).

²⁴ G. K. White, *Proc. Phys. Soc. (London)* **A66**, 559 (1953).

Table I the ratio $\kappa\rho_0/T$ decreases with decreasing temperature. At 150°K, $\kappa\rho_0/T$ is close to the theoretical value given by the Lorentz number, $L_0=2.45 \times 10^{-8}$ V²/deg², which is calculated under the assumption that the conduction electrons are scattered elastically. The scattering of electrons by static lattice imperfections such as vacancies is expected to be elastic. Therefore, the Wiedemann-Franz law should be valid for the electron scattering caused by vacancies.

In order to account for the deviation from the Wiedemann-Franz law, mentioned above, the function G , defined in Eq. (11), was replaced by the function

$$G' = \frac{S_e^0}{(\rho_0/\Delta\rho)(L_0T/\kappa\rho_0)+1}, \quad (25)$$

where the ratio $L_0T/\kappa\rho_0$ was taken from Table I. Using the corrected function G' from Eq. (25) the electronic component ΔS_e and the phonon-drag component ΔS_g were calculated again from the data of Fig. 4. The results are shown in Figs. 8 and 9, respectively. The phonon-drag component ΔS_g at 20 and at 40°K,

TABLE I. Temperature dependence of the Wiedemann-Franz ratio $\kappa\rho_0/T$ for gold. L_0 is the Lorentz number: $L_0=2.45 \times 10^{-8}$ (V/deg)². The values are obtained from the thermal conductivity data of Ref. 24 and from the electrical resistivity of the annealed specimen of the present investigation.

| T(°K) | 20 | 30 | 40 | 50 | 60 | 70 | 80 | 100 | 150 |
|---------------------|------|------|------|------|------|------|------|------|------|
| $\kappa\rho_0/TL_0$ | 0.40 | 0.53 | 0.62 | 0.68 | 0.73 | 0.77 | 0.82 | 0.90 | 0.99 |

calculated with G' from Eq. (25), is shown in Fig. 10 as a function of the quenched-in electrical resistivity.

V. DISCUSSION

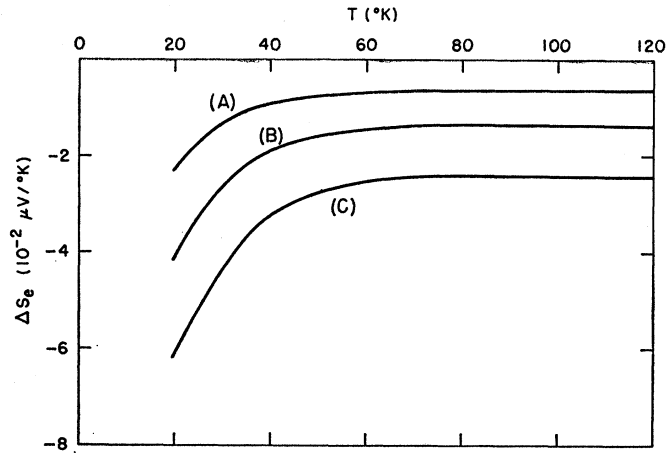
At temperatures below approximately $\theta/10$ (θ = Debye temperature) the thermoelectric behavior of the noble metals is generally influenced to a large extent by very small traces of transition metal impurities such as iron present in solid solution.^{21,25,26} The sharp drop of the thermoelectric power of the specimen wire with decreasing temperature at about 10°K to negative values (Fig. 1) may be caused mainly by traces of iron in the material. By introducing lattice vacancies into the metal the contribution which causes the negative thermoelectric power below 10°K is reduced, thus resulting in a positive value of ΔS at temperatures below 10°K (Figs. 4 and 7). Beyond this remark we refrain from a further analysis of the data at temperatures below 20°K.

As mentioned in Sec. IIIB, the temperature of the upper junction of the specimen wires rose slightly above the temperature of the cooling bath after heating the lower junction. The values of $|\Delta S|$ obtained above 20°K with liquid helium as cooling medium are, therefore, somewhat too large. At 60°K the error of ΔS ,

²⁵ W. B. Pearson, *Phys. Rev.* **119**, 549 (1960).

²⁶ A. Kjekshus and W. B. Pearson, *Can. J. Phys.* **40**, 98 (1962).

FIG. 8. Change of the electronic thermoelectric power of gold caused by quenched-in vacancies as function of temperature. (A): $c=0.403 \times 10^{-2}$ at. %; (B): $c=0.865 \times 10^{-2}$ at. %; (C): $c=1.42 \times 10^{-2}$ at. %. The curves are corrected for deviations from the Wiedemann-Franz law.



calculated from the temperature shift measured with an annealed specimen, is about 20%. However, the actual error of ΔS , caused by the temperature shift in the quenched specimens, is somewhat smaller since the heat conductivity of the specimen wire is reduced due to the quenched-in defects. The relative error introduced by the temperature shift decreases with decreasing temperature because of the increasing value of $|\Delta S|$. In the experiments with liquid nitrogen as cooling medium this error of ΔS is 1%.

A. Electronic Component of ΔS

Polák^{26a,26b} measured the change ΔS of the thermoelectric power of gold wires due to quenching in the

temperature range between 78° and 293°K. Polák determined the quenched-in electrical resistance at room temperature. This author also found that vacancies reduce the thermoelectric power of gold and that ΔS is independent of the temperature for temperatures above about 150°K. Using a monovacancy resistivity of $1.8 \times 10^{-6} \Omega \text{ cm/at. \%}$, for 200°K, the relation $(\Delta S/c)_{200^{\circ}K} = -1.30 \mu V/^{\circ}K \text{ at. \%}$ is obtained from Polák's data. The difference between this change of the electronic thermoelectric power per vacancy measured by Polák and the value given in Eq. (24) may be partly due to deviations from Matthiessen's rule which yield, as mentioned in Sec. IV, at room temperature, a larger resistance increment due to quenching than at 4.2°K.

The change of the electronic component of the thermoelectric power caused by lattice vacancies has

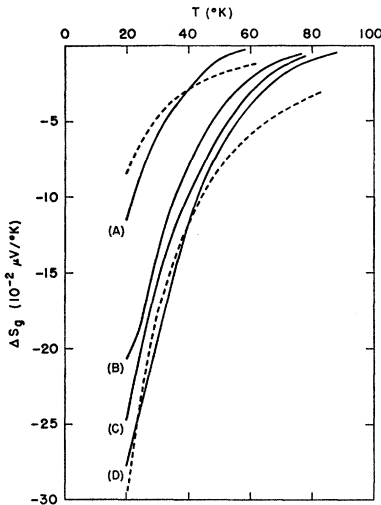


FIG. 9. Change of the phonon-drag thermoelectric power of gold caused by quenched-in vacancies as function of temperature. (A): $c=0.403 \times 10^{-2}$ at. %; (B): $c=0.825 \times 10^{-2}$ at. %; (C): $c=0.865 \times 10^{-2}$ at. %; (D): $c=1.42 \times 10^{-2}$ at. %. The curves are corrected for deviations from the Wiedemann-Franz law. The dashed curves are calculated from Eq. (36) and are adjusted at 40°K to the experimental values of ΔS_p .

^{26a} J. Polák, Czech. J. Phys. B13, 616 (1963).

^{26b} J. Polák, Czech. J. Phys. B14, 176 (1964).

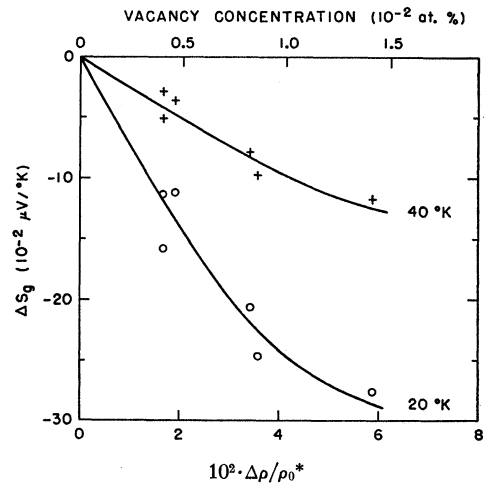


FIG. 10. Change of the phonon-drag thermoelectric power of gold at 20 and 40°K due to quenching versus the quenched-in electrical resistivity. ρ_0^* is the annealed resistivity at 77.3°K. The data are corrected for deviations from the Wiedemann-Franz law.

been calculated by Abelès²⁷ for gold and by Blatt^{28,29} for copper. Both authors used the free-electron approximation. Abelès represented the vacant lattice site by a repulsive square-well potential whose radius was taken as the atomic radius of the metal and whose height was adjusted in order to satisfy the Friedel sum rule.³⁰ Blatt used the negative of the Hartree potential of the free copper ion and adjusted the screening charge distribution until the Friedel sum rule was satisfied. Taking the value of the derivative $(\partial/\partial E)(\ln\Delta\rho)$ obtained by Abelès,²⁷ in the limit of small vacancy concentrations the relation $(\Delta S_e/c)_{200^\circ\text{K}} = -2.07 \mu\text{V}/^\circ\text{K}$ at $\%_0$ is calculated from Eq. (10). This result is, perhaps fortuitously, in good agreement with the experimental value presented in Eq. (24). In the limit of small vacancy concentrations Blatt^{28,29} found at room temperature for vacancies in copper the relation $\Delta S_e/c \approx -1.0 \mu\text{V}/^\circ\text{K}$ at $\%_0$.

B. Phonon Drag Component of ΔS

The experimental results on the phonon drag component ΔS_g can be analyzed using Eq. (18). To simplify the calculation we drop the differentiation between phonons with different polarization j . Therefore, we omit hereafter the parameter j and replace sums over j by the factor of 3. In the integration over all phonons the phonon spectrum is cut off at the Debye frequency. Further we neglect dispersion. Using these approximations we can estimate the relaxation time $\tau_i(\mathbf{q})$ from the experimentally obtained phonon-drag component ΔS_g with Eq. (18) after determining the functions $\tau_0(\mathbf{q})$ and $s_g(\mathbf{q})$ independently.

The relaxation time $\tau_0(\mathbf{q})$ of the phonon scattering in the host material may be estimated from the experimentally determined lattice thermal conductivity of pure gold. In the Debye approximation the lattice thermal conductivity K of an isotropic crystal is given by the following equation^{31,32}:

$$K = \frac{k_B}{2\pi^2 v_s} \left(\frac{k_B T}{\hbar} \right)^3 \int_0^{\theta/T} dz \tau_0(z) \frac{z^4 e^z}{(e^z - 1)^2}. \quad (26)$$

The parameter z is defined by Eq. (20). v_s is the sound velocity, θ the Debye temperature. The lattice thermal conductivity K of gold has been determined from heat conductivity measurements with dilute gold-iron alloys.³³ For gold K has been found to pass through a maximum at about 20°K and to follow the relation

$$KT = 8 \text{ W/cm} \quad (27)$$

at temperatures above 30°K .

²⁷ M. F. Abelès, *Compt. Rend.* **237**, 796 (1953).

²⁸ F. J. Blatt, *Phys. Rev.* **100**, 666 (1955).

²⁹ F. J. Blatt, *Phys. Rev.* **103**, 1905 (1956).

³⁰ J. Friedel, *Phil. Mag.* **43**, 153 (1952).

³¹ P. G. Klemens, in *Solid State Physics*, edited by F. Seitz and D. Turnbull (Academic Press Inc., New York, 1958), Vol. 7, p. 1.

³² J. Callaway, *Phys. Rev.* **113**, 1046 (1959).

³³ G. K. White, S. B. Woods, and M. T. Elford, *Phil. Mag.* **4**, 688 (1959).

In pure gold, phonons are scattered dominantly by phonon-phonon interactions at temperatures above 30°K . The relaxation time $\tau_0(\mathbf{q})$ at temperatures above 30°K can be estimated by finding the proper function $\tau_0(z)$ in Eq. (26) which yields the relation (27). A good fit of the relation (27) was obtained using in Eq. (26) the relaxation time

$$\tau_0^{-1} = b\omega^2 T e^{-\beta/T}, \quad (28)$$

with $b = 6.96 \times 10^{-18} \text{ sec/deg}$ and $\beta = 22^\circ\text{K}$. The integration was carried out with a CDC-3600 computer. In the calculation a Debye temperature of³⁴ $\theta = 164.5^\circ\text{K}$ and a sound velocity of³⁵ $v_s = 3.217 \times 10^5 \text{ cm/sec}$ were used. A relaxation time similar to that given in Eq. (28) has been calculated by Walker and Pohl³⁶ and by Walker³⁷ in an attempt to fit their data on the thermal conductivity of the alkali halides which show a T^{-1} proportionality at high temperatures.

The function $s_g(\mathbf{q})$ may be estimated from Bailyn's expression for the phonon-drag thermoelectric power given above. From Eqs. (19) and (23) we find by replacing the summation over \mathbf{q} by an integral

$$S_g^0 \sim T^3 \sum_{\mathbf{k}\mathbf{k}'}^{[\mathbf{q}]} \int_0^{\theta/T} dz \frac{z^4 e^z}{(e^z - 1)^2} \alpha(\mathbf{q}; \mathbf{k}, \mathbf{k}') (\mathbf{q} + \mathbf{K}). \quad (29)$$

At temperatures above 30°K , where the lattice thermal conductivity of gold is proportional to T^{-1} , the relative transition probability defined in Eq. (21) is given by

$$\alpha(\mathbf{q}; \mathbf{k}, \mathbf{k}') = \tau_0(\mathbf{q}) / \tau_{ep}(\mathbf{k}, \mathbf{k}'). \quad (30)$$

With Eq. (30) and with $\tau_0(\mathbf{q})$ from Eq. (28) we obtain from Eq. (29)

$$S_g^0 \sim e^{\beta/T} \sum_{\mathbf{k}\mathbf{k}'}^{[\mathbf{q}]} \int_0^{\theta/T} dz \frac{z^2 e^z}{(e^z - 1)^2} \frac{\mathbf{q} + \mathbf{K}}{\tau_{ep}(\mathbf{k}, \mathbf{k}')}. \quad (31)$$

The factor $(\mathbf{q} + \mathbf{K}) / \tau_{ep}(\mathbf{k}, \mathbf{k}')$ within the integral, which depends on the electron-phonon interaction, is difficult to evaluate. Treating this factor as an adjustable constant we find

$$S_g^0 = A e^{\beta/T} \int_0^{\theta/T} dz \frac{z^2 e^z}{(e^z - 1)^2}. \quad (32)$$

By adjusting this expression to the experimental value of S_g^0 at 40°K the factor A is found to be

$$A = 0.166 \mu\text{V}/^\circ\text{K}. \quad (33)$$

Using this value of A , Eq. (32) approximates the experimentally determined temperature dependence of S_g^0 , indicated in Fig. 1, within 15% in the temperature range between 30 and 80°K . The values of the transport integral in Eq. (32) were obtained from Rogers and Powell.³⁸

³⁴ J. R. Neighbours and G. A. Alers, *Phys. Rev.* **111**, 707 (1958).

³⁵ H. V. Bohm and V. J. Easterling, *Phys. Rev.* **128**, 1021 (1962).

³⁶ C. T. Walker and R. O. Pohl, *Phys. Rev.* **131**, 1433 (1963).

³⁷ C. T. Walker, *Phys. Rev.* **132**, 1963 (1963).

³⁸ W. M. Rogers and R. L. Powell, *Tables of Transport Integrals*, Natl. Bur. Std. (U.S.) Circ. **595** (1958).

According to Eqs. (16), (32), and (33) the function $s_\theta(\mathbf{q})$ is given by

$$s_\theta = \frac{(0.166 \mu\text{V}/^\circ\text{K}) \left(\frac{\hbar v_s}{k_B T} \right)^3 e^{\beta/T} e^{\epsilon}}{4\pi (e^\epsilon - 1)^2}. \quad (34)$$

After the determination of the functions $\tau_0(\mathbf{q})$ and $s_\theta(\mathbf{q})$, the relaxation time $\tau_i(\mathbf{q})$ can be estimated from the experimentally determined phonon-drag component ΔS_θ with Eq. (18). Assuming a pure Rayleigh-type mechanism for the scattering of phonons by vacancies, $\tau_i(\mathbf{q})$ has the form

$$\tau_i^{-1} = a\omega^4. \quad (35)$$

Inserting Eqs. (28), (34), and (35) into Eq. (18) we obtain

$$\Delta S_\theta = -0.166 \times e^{\beta/T} \int_0^{\theta/T} dz \frac{z^2 e^z}{(e^z - 1)^2} \times \left[1 / \left(1 + \frac{\hbar^2 e^{-\beta/T}}{a k_B^2 z^2 T} \right) \right] [\mu\text{V}/^\circ\text{K}]. \quad (36)$$

With Eq. (36) the parameter a was determined from each experimental value of ΔS_θ at 40°K shown in Fig. 9. Using this value of a the phonon drag component ΔS_θ was calculated from Eq. (36) as a function of the temperature. The integration was carried out with a CDC-3600 computer. The results are shown in Fig. 9 by a dashed line for two vacancy concentrations. The temperature dependence of ΔS_θ calculated from Eq. (36) is in qualitative agreement with the experimental results.

Using the data on the phonon-drag component ΔS_θ at 40°K, presented in Fig. 10, the value

$$a/c = (20 \pm 6) \times 10^{-42} \text{ sec}^3/\text{at. } \%. \quad (37)$$

was calculated from Eq. (36).

A theoretical treatment of the scattering of phonons by point defects has been given by Klemens³⁹ using second-order perturbation theory. The calculation was carried out for a cubic crystal and for phonons of lowest frequency neglecting dispersion. Trigonometric ratios were replaced by root-mean-square values. Klemens obtained a Rayleigh-type scattering law, shown in Eq. (35), with a scattering parameter

$$a = (3\Delta_0 c / \pi v_s^3) L^2, \quad (38)$$

where

$$L^2 = \frac{1}{12} \left(\frac{\Delta M}{M} \right)^2 + \left[\frac{1}{\sqrt{6}} \frac{\Delta F}{F} - \left(\frac{2}{3} \right)^{1/2} Q \gamma \frac{\Delta R}{R} \right]^2. \quad (39)$$

Here Δ_0 is the atomic volume of the crystal, c the mole fraction of the point defects, v_s the sound velocity and γ the Grüneisen constant. M is the atomic mass of the crystal, F the force constant of a linkage, R the nearest neighbor distance, and ΔM , ΔF , and ΔR are the changes in them at the location of the point defect. ΔF is positive

if the force constant of the nearest linkages is higher than normal. ΔR is positive if the nearest neighbors are displaced outwards. The constant Q contains the contribution to the scattering matrix from the strains in the lattice outside the six nearest neighbors of the point defect.

In the case of a vacancy we have $\Delta M/M = -1$, $\Delta F/F = -1$, and $Q = 3.2$.³⁹ To estimate ΔR we assume that the interionic distance is the sum of the ionic radii, so that ΔR is the difference between the radii of a vacancy and a gold ion. From the activation volume for vacancy formation in gold^{17,40} we obtain $\Delta R/R = -0.095$. With the Grüneisen constant of gold⁴¹ $\gamma = 3.03$ we find from Eqs. (38) and (39)

$$a/c = 1.01 \times 10^{-42} \text{ sec}^3/\text{at. } \%. \quad (40)$$

The Rayleigh scattering parameter calculated from Klemens' theory is by an order of magnitude smaller than the value given in Eq. (37). The contribution of the mass difference term to the scattering parameter given in Eq. (40) is by a factor of about 40 smaller than the value shown in Eq. (37). This result indicates that phonons are scattered by vacancies predominantly through the strain field associated with the vacant lattice site, in agreement with recent measurements of the phonon scattering by F centers³⁷ and chemical impurities^{36,42} in alkali halides.

The Rayleigh scattering parameter calculated from the phonon-drag component of ΔS is in reasonable agreement with the value derived from Carruthers'⁴³ theory of the strain field scattering of an imperfection. Carruthers obtained for the relaxation time of the phonon scattering by the strain field associated with a point defect an expression of the form given in Eqs. (35) and (38) with

$$L^2 = 80\gamma^2 \epsilon^2. \quad (41)$$

The parameter ϵ describes the displacement of the nearest neighbors of the impurity and is equal to the ratio $\Delta R/R$ which appears in Klemens' theory. The scattering parameter calculated from Eqs. (38) and (41) with the value of the ratio $\Delta R/R$ given above is $a/c = 33 \times 10^{-42} \text{ sec}^3/\text{at. } \%$.

ACKNOWLEDGMENTS

The successful completion of this work is due in large part to the valuable assistance of R. E. Govednik during the experiments. Some parts of the work were carried out by R. E. Hetric, student aide during the summer of 1963. The programming of the calculations on the IBM-704 and CDC-3600 was done by J. M. Heestand, A. H. Lent, and A. J. Strecok. The author is grateful to Dr. J. E. Robinson for valuable discussions.

⁴⁰ H. H. Grimes (to be published).

⁴¹ N. F. Mott and H. Jones, *The Theory of the Properties of Metals and Alloys* (Dover Publications, Inc., New York, 1958), p. 319.

⁴² M. V. Klein, *Phys. Rev.* **123**, 1977 (1961).

⁴³ P. Carruthers, *Rev. Mod. Phys.* **33**, 92 (1961), Eq. (4.43).

³⁹ P. G. Klemens, *Proc. Phys. Soc. (London)* **A68**, 1113 (1955).